

# FedBiCross: A Bi-Level Optimization Framework to Tackle Non-IID Challenges in Data-Free One-Shot Federated Learning on Medical Data

Yuexuan Xia<sup>1,\*</sup>, Yinghao Zhang<sup>2,\*†</sup>, Yalin Liu<sup>2</sup>, Hong-Ning Dai<sup>3</sup>, Yong Xia<sup>1,†</sup>

<sup>1</sup> School of Computer Science and Engineering, Northwestern Polytechnical University, China

<sup>2</sup> School of Science and Technology, Hong Kong Metropolitan University, Hong Kong

<sup>3</sup> Department of Computer Science, Hong Kong Baptist University, Hong Kong

**Abstract**—Data-free knowledge distillation-based one-shot federated learning (OSFL) trains a model in a single communication round without sharing raw data, making OSFL attractive for privacy-sensitive medical applications. However, existing methods aggregate predictions from all clients to form a global teacher. Under non-IID data, conflicting predictions cancel out during averaging, yielding near-uniform soft labels that provide weak supervision for distillation. We propose FedBiCross, a personalized OSFL framework with three stages: (1) clustering clients by model output similarity to form coherent sub-ensembles, (2) bi-level cross-cluster optimization that learns adaptive weights to selectively leverage beneficial cross-cluster knowledge while suppressing negative transfer, and (3) personalized distillation for client-specific adaptation. Experiments on four medical image datasets demonstrate that FedBiCross consistently outperforms state-of-the-art baselines across different non-IID degrees.

**Index Terms**—Data heterogeneity, one-shot federated learning, medical image analysis, personalization.

## I. INTRODUCTION

Federated learning (FL) [1] enables collaborative model training while keeping raw data local, which is particularly valuable for medical applications where patient privacy is paramount. However, conventional FL methods require repeated communication rounds, which becomes problematic in medical settings: hospital networks often operate offline with regulated data transfer procedures, privacy policies may restrict data access to short windows, and frequent communication enlarges attack surfaces.

These constraints motivate one-shot federated learning (OSFL) [2], where each client uploads its model only once and the server trains a global model without accessing raw data. Data-free knowledge distillation (DFKD) methods [3]–[5] are particularly attractive for OSFL because they synthesize data directly from uploaded client models and thus avoid both transmitting data-dependent surrogates and uploading additional generative models, reducing privacy exposure and communication overhead. Specifically, DFKD-based OSFL methods leverage techniques such as DeepInversion [6] to invert client models: the server forms an ensemble teacher from client predictions, generates synthetic images by optimizing random noise to match the ensemble’s batch normalization statistics, and distills the ensemble’s knowledge into a student

model. However, this approach faces a fundamental limitation under non-IID distributions prevalent in medical data. Under non-IID distributions, each client is trained predominantly on a subset of classes, causing its model to become biased toward locally frequent categories. Consequently, for the same synthetic input, different clients produce conflicting predictions based on their respective biases. When these predictions are averaged to form an ensemble teacher, the probability mass disperses across multiple classes, yielding near-uniform soft labels that provide negligible supervisory signal for DFKD.

To address the teacher disagreement problem, a natural solution is to cluster similar clients to form coherent sub-ensembles. However, this introduces a new challenge: **balancing intra-cluster and cross-cluster knowledge**. Intra-cluster knowledge, derived from a cluster-specific ensemble teacher and its synthetic data, provides consistent supervision but is limited in quantity and can lead to overfitting. Cross-cluster knowledge increases data diversity, yet it may also introduce distribution shift and negative transfer when the source domains are incompatible. The key question becomes: *how to selectively leverage cross-cluster knowledge to enhance intra-cluster learning while suppressing harmful transfer?*

To address these challenges, we propose **FedBiCross**, a personalized one-shot FL framework. Our key insight is that clients with similar local data distributions tend to produce consistent predictions, so grouping them into coherent sub-ensembles can yield peaked and confident soft labels for effective distillation. Furthermore, while intra-cluster knowledge alone may lead to overfitting due to limited synthetic data, cross-cluster knowledge can serve as a valuable source of diversity—provided that harmful transfer from incompatible clusters is suppressed. This motivates a bi-level optimization scheme that learns adaptive cross-cluster weights by evaluating their contribution to target-cluster performance. Finally, to bridge the gap between cluster-level and client-level distributions, we introduce personalized distillation that adapts cluster models to individual clients. Our main contributions are:

- We propose a client clustering strategy based on model output similarity, which groups clients into coherent sub-ensembles to mitigate the teacher disagreement problem caused by conflicting predictions under non-IID settings.
- We introduce a bi-level cross-cluster optimization frame-

\*Equal contributions. †Corresponding authors.

work that learns adaptive cross-cluster weights, enabling selective utilization of beneficial cross-cluster knowledge while suppressing negative transfer.

- We develop a personalized distillation stage that adapts cluster-level models to individual clients, capturing client-specific patterns while preserving cross-cluster knowledge from cross-cluster optimization.

## II. RELATED WORKS

### A. Personalized Federated Learning

FL [1] enables collaborative training without sharing raw data, but a single global model can be suboptimal under statistical heterogeneity [7]. Personalized FL (pFL) addresses this via, e.g., local fine-tuning [8], model interpolation [9], and clustering-based training [10]–[12]. Clustering-based pFL is particularly suitable for large-scale systems, as it groups clients with similar distributions and learns one model per cluster. IFCA [11] iteratively assigns clients and updates cluster models. CFL [10] clusters clients by hierarchical clustering of local updates. PACFL [12] scales clustering by estimating distribution similarity from compact subspace signatures.

### B. One-Shot Federated Learning

OSFL aims to achieve effective aggregation with minimal communication and is typically categorized into three approaches. Auxiliary dataset-based methods [2] distill using server-side data, but distribution matching is difficult for medical data and may raise privacy concerns. Data transmission-based methods upload data-dependent surrogates such as distributions [13], intermediate features [14], or distilled samples [15], yet privacy risks persist. Generative model-based methods synthesize data on the server, and some additionally require uploading client-trained generative models [16], [17], which increases communication overhead. To address this, DFCD-based methods [3]–[5] synthesize samples directly from uploaded client models using DeepInversion-style optimization and distill them to transfer knowledge into the global model. DENSE [3] enhances transferability by generating diverse boundary samples but may underperform on complex medical distributions. FedISCA [4] improves robustness by leveraging the full synthesis trajectory from noise to realistic images and applying noise-adapted batch normalization. Co-Boosting [5] alternates hard-sample synthesis and client-wise teacher ensemble reweighting.

## III. METHODOLOGY

In this section, we introduce **FedBiCross**, a framework for personalized OSFL. Fig. 1 illustrates the overall framework and Algorithm 1 summarizes the procedure. FedBiCross consists of three stages: (1) *client clustering and cluster-specific data generation*, (2) *bi-level cross-cluster optimization*, and (3) *personalized distillation* to fine-tune models for each client.

### A. Stage 1: Client Clustering and Data Generation

1) *Client Clustering via Similarity*: The effectiveness of knowledge distillation relies on the teacher providing confident and consistent soft labels. When client models disagree, their conflicting predictions cancel out during averaging, producing near-uniform distributions that provide negligible supervision.

To address this, we group clients whose models produce similar predictions. Specifically, the server generates a set of  $M$  random noise images  $\{\mathbf{z}_m\}_{m=1}^M$  and computes predictions from each client model:  $\mathbf{p}_i = [f_i(\mathbf{z}_1), \dots, f_i(\mathbf{z}_M)] \in \mathbb{R}^{M \times C}$ , where  $C$  is the number of classes and  $f_i$  is the local model. We apply  $K$ -means clustering on the prediction matrices:  $\min_{\{\mathcal{C}_k\}, \{\mathbf{c}_k\}} \sum_{k=1}^K \sum_{i \in \mathcal{C}_k} \|\mathbf{p}_i - \mathbf{c}_k\|_F^2$ , where  $\|\cdot\|_F$  denotes the Frobenius norm,  $\{\mathcal{C}_k\}_{k=1}^K$  are the resulting clusters, and  $\mathbf{c}_k$  denotes the centroid of cluster  $k$ . For each cluster  $k$ , we construct an ensemble teacher via:  $F_k(\mathbf{x}) = \frac{1}{|\mathcal{C}_k|} \sum_{i \in \mathcal{C}_k} f_i(\mathbf{x})$ .

2) *Trajectory-Based Synthesis*: For each cluster  $k$ , we generate synthetic data via Deep Inversion over  $T$  iterations with batch size  $B$ . Let  $\hat{\mathbf{x}}_k^{(0)}$  be the initial random noise. At each iteration  $t \in \{1, \dots, T\}$ , we update:

$$\hat{\mathbf{x}}_k^{(t)} = \hat{\mathbf{x}}_k^{(t-1)} - \eta_s \nabla_{\hat{\mathbf{x}}} \mathcal{L}_{\text{DI}}(\hat{\mathbf{x}}_k^{(t-1)}; F_k, y), \quad (1)$$

where  $\eta_s$  is the synthesis learning rate and  $y$  is the target class label for the synthetic sample, which is uniformly sampled from all classes to ensure balanced generation. The Deep Inversion loss [4] is defined as:  $\mathcal{L}_{\text{DI}}(\hat{\mathbf{x}}; F, y) =$

$$\mathcal{L}_{\text{CE}}(F(\hat{\mathbf{x}}), y) + \alpha_{\text{TV}} \mathcal{R}_{\text{TV}}(\hat{\mathbf{x}}) + \alpha_{\text{BN}} \mathcal{R}_{\text{BN}}(\hat{\mathbf{x}}), \quad (2)$$

where  $\mathcal{L}_{\text{CE}}$ ,  $\mathcal{R}_{\text{TV}}$  and  $\mathcal{R}_{\text{BN}}$  are cross-entropy, total variation, and BN losses, and  $\alpha_{\text{TV}}$  and  $\alpha_{\text{BN}}$  are hyper-parameters.

A key limitation of standard Deep Inversion is that using only the final synthesized images for knowledge distillation may lead to overfitting due to limited data diversity. To address this, we leverage the full synthesis trajectory  $\{\hat{\mathbf{x}}_k^{(t)}\}_{t=1}^T$  as training sources to augment data diversity.

3) *Noise-Adapted Teachers*: The teacher’s BN statistics are calibrated for real images, causing unreliable predictions when early-stage noisy samples are fed in. We construct a noise-adapted teacher  $\tilde{F}_k$  by traversing the stored trajectory in reverse order and progressively updating the noise-adapted statistics  $(\tilde{\mu}_k, \tilde{\sigma}_k^2)$ . For  $t = 1, \dots, T$ , we have:

$$\begin{aligned} \tilde{\mu}_k &\leftarrow \beta \tilde{\mu}_k + (1 - \beta) \mu(\hat{\mathbf{x}}_k^{(T-t+1)}), \\ \tilde{\sigma}_k^2 &\leftarrow \beta \tilde{\sigma}_k^2 + (1 - \beta) \sigma^2(\hat{\mathbf{x}}_k^{(T-t+1)}), \end{aligned} \quad (3)$$

where  $(\tilde{\mu}_k, \tilde{\sigma}_k^2)$  are initialized from the original BN statistics and  $\beta$  is the momentum. This yields a noise-adapted teacher  $\tilde{F}_k$  that provides reliable supervision across all noise levels.

### B. Stage 2: Bi-Level Cross-Cluster Optimization

While clustering produces coherent teachers, intra-cluster data alone leads to overfitting. Incorporating cross-cluster data can improve diversity, but risks **negative transfer** from incompatible distributions.

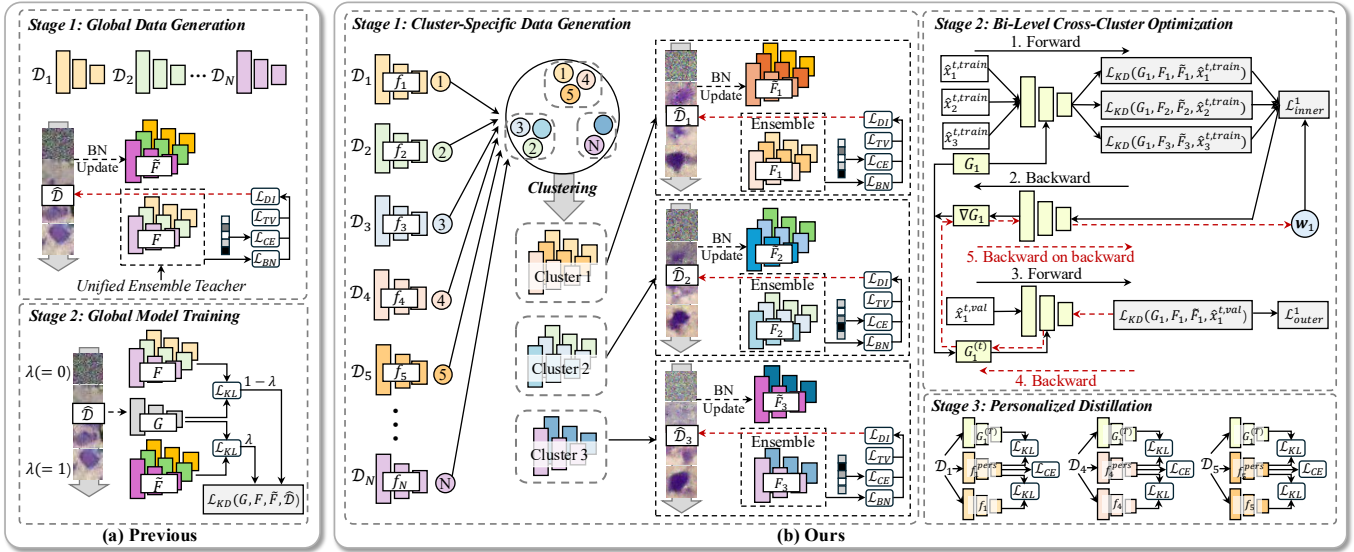


Fig. 1. Overview of FedBiCross. (a) Previous methods (e.g., FedISCA [4]) construct a unified ensemble teacher from all clients, ignoring distribution heterogeneity. (b) Our approach consists of three stages: **Stage 1** clusters clients by model output similarity and generates cluster-specific synthetic data; **Stage 2** performs bi-level optimization to learn adaptive cross-cluster weights; **Stage 3** personalizes models for individual clients via local fine-tuning.

1) *Problem Formulation*: Our key insight is that **the usefulness of cross-cluster knowledge should be measured by its effect on the target cluster’s performance**. This naturally leads to a bi-level optimization formulation: the *inner level* trains the cluster model using weighted cross-cluster data, while the *outer level* evaluates the resulting model on the target cluster’s validation set and adjusts the weights accordingly.

To enable this, we partition synthetic samples into training and validation subsets via a fixed index partition  $\mathcal{I}^{\text{train}} \cup \mathcal{I}^{\text{val}} = \{1, \dots, B\}$  with  $\mathcal{I}^{\text{train}} \cap \mathcal{I}^{\text{val}} = \emptyset$ .

Formally, for each cluster  $k$ , we introduce learnable cross-cluster weights  $\mathbf{w}_k = (w_{k,1}, \dots, w_{k,K})^\top$ , where  $w_{k,j} \geq 0$ ,  $\sum_{j=1}^K w_{k,j} = 1$ , and  $w_{k,j}$  represents the contribution of cluster  $j$ ’s knowledge to training cluster  $k$ ’s model. Let  $G_k$  denote the cluster model for cluster  $k$ . We formulate the following bi-level optimization problem over the entire synthesis trajectory:

$$\mathbf{w}_k^* = \underset{\mathbf{w}_k}{\operatorname{argmin}} \sum_{t=1}^T \mathcal{L}_{\text{KD}}^{(t)}(G_k^*(\mathbf{w}_k), F_k, \tilde{F}_k, \hat{\mathbf{x}}_k^{(t,\text{val})})$$

$$\text{s.t. } G_k^*(\mathbf{w}_k) = \underset{G}{\operatorname{argmin}} \sum_{t=1}^T \sum_{j=1}^K w_{k,j} \cdot \mathcal{L}_{\text{KD}}^{(t)}(G, F_j, \tilde{F}_j, \hat{\mathbf{x}}_j^{(t,\text{train})}), \quad (4)$$

where the knowledge distillation loss is:  $\mathcal{L}_{\text{KD}}^{(t)}(G, F, \tilde{F}, \hat{\mathbf{x}}) =$

$$\lambda^{(t)} \cdot \text{KL}(\tilde{F}(\hat{\mathbf{x}}) \| G(\hat{\mathbf{x}})) + (1 - \lambda^{(t)}) \cdot \text{KL}(F(\hat{\mathbf{x}}) \| G(\hat{\mathbf{x}})), \quad (5)$$

with  $\lambda^{(t)} = 1 - t/T$  decreasing over iterations, so that early noisy samples rely more on the noise-adapted teacher  $\tilde{F}$  while later realistic samples use the original teacher  $F$ .

The **inner optimization** trains  $G_k$  on a weighted mixture of all clusters’ synthetic data across all iterations, where  $w_{k,j}$  controls how much cluster  $j$  contributes. The **outer optimization** evaluates how well this trained model performs

on cluster  $k$ ’s own validation data aggregated over the entire trajectory, and adjusts the weights to minimize the total validation loss. Through this feedback loop, clusters providing beneficial knowledge will have their weights increased.

2) *Online Optimization*: The bi-level problem in Eq. (4) aggregates losses over the entire trajectory  $\{\hat{\mathbf{x}}_k^{(t)}\}_{t=1}^T$ , requiring all synthetic data to be available before optimization. However, the synthesis process (Eq. 1) generates data sequentially—each  $\hat{\mathbf{x}}_k^{(t)}$  depends on  $\hat{\mathbf{x}}_k^{(t-1)}$ —making it natural to optimize incrementally as data becomes available.

We therefore reformulate Eq. (4) as an **online bi-level optimization** problem. At each synthesis iteration  $t$ , given the newly generated samples  $\{\hat{\mathbf{x}}_j^{(t)}\}_{j=1}^K$ , we update the cross-cluster weights and cluster model by solving:

$$\mathbf{w}_k^{(t)} = \underset{\mathbf{w}_k}{\operatorname{argmin}} \mathcal{L}_{\text{KD}}^{(t)}(G_k^{(t)}(\mathbf{w}_k), F_k, \tilde{F}_k, \hat{\mathbf{x}}_k^{(t,\text{val})})$$

$$\text{s.t. } G_k^{(t)}(\mathbf{w}_k) = \underset{G}{\operatorname{argmin}} \sum_{j=1}^K w_{k,j} \cdot \mathcal{L}_{\text{KD}}^{(t)}(G, F_j, \tilde{F}_j, \hat{\mathbf{x}}_j^{(t,\text{train})}), \quad (6)$$

where  $G_k^{(t)}$  and  $\mathbf{w}_k^{(t)}$  are initialized from their previous values  $G_k^{(t-1)}$  and  $\mathbf{w}_k^{(t-1)}$ . By accumulating updates over  $t = 1, \dots, T$ , the online procedure approximates the original objective in Eq. (4). Since solving Eq. (6) exactly at each iteration is still expensive, we further approximate it with single-step gradient updates:

**Inner Update**. Given the current cross-cluster weights  $\mathbf{w}_k^{(t-1)}$ , we update the cluster model using weighted cross-cluster knowledge on the training split:  $G_k^{(t)} = G_k^{(t-1)} -$

$$\eta_G \nabla_G \sum_{j=1}^K w_{k,j}^{(t-1)} \cdot \mathcal{L}_{\text{KD}}^{(t-1)}(G_k^{(t-1)}, F_j, \tilde{F}_j, \hat{\mathbf{x}}_j^{(t-1,\text{train})}), \quad (7)$$

where  $\eta_G$  is the learning rate for the cluster model.

**Outer Update.** The cross-cluster weights are updated based on validation performance of the updated model:

$$\mathbf{w}_k^{(t)} = \mathbf{w}_k^{(t-1)} - \eta_w \nabla_{\mathbf{w}} \mathcal{L}_{\text{KD}}^{(t-1)}(G_k^{(t)}, F_k, \tilde{F}_k, \hat{\mathbf{x}}_k^{(t-1, \text{val})}), \quad (8)$$

where  $\eta_w$  is the learning rate for the weights. After each update, we project  $\mathbf{w}_k^{(t)}$  onto the probability simplex to ensure  $w_{k,j}^{(t)} \geq 0$  and  $\sum_{j=1}^K w_{k,j}^{(t)} = 1$ .

This online scheme can be viewed as stochastic approximation to the batch objective in Eq. (4), where each iteration provides an unbiased gradient estimate. By coupling weight learning with the synthesis trajectory, the cross-cluster weights are progressively refined: early iterations explore different cross-cluster combinations, while later iterations consolidate beneficial knowledge transfer patterns.

### C. Stage 3: Personalized Knowledge Distillation

After  $T$  iterations, we obtain cluster models  $\{G_k^{(T)}\}$  that capture cluster-level knowledge through cross-cluster optimization. Since clients within the same cluster may still exhibit heterogeneous data distributions that the cluster model cannot fully capture, we further personalize it for each individual client using their private local data. For client  $i$  belonging to cluster  $\mathcal{C}_k$ , we initialize a personalized model  $f_i^{\text{pers}}$  from the cluster model  $G_k^{(T)}$  and fine-tune it by minimizing the following loss function:  $\mathcal{L}_{\text{pers}} = \mathcal{L}_{\text{CE}}(f_i^{\text{pers}}(\mathbf{x}), y) +$

$$\gamma \cdot \text{KL}(G_k^{(T)}(\mathbf{x}) \parallel f_i^{\text{pers}}(\mathbf{x})) + \delta \cdot \text{KL}(f_i(\mathbf{x}) \parallel f_i^{\text{pers}}(\mathbf{x})), \quad (9)$$

where  $(\mathbf{x}, y) \in \mathcal{D}_i$  denotes samples from client  $i$ 's local dataset. The three terms serve complementary purposes: (1) the cross-entropy loss  $\mathcal{L}_{\text{CE}}$  trains the model to fit the client's local data distribution; (2) the KL divergence from the cluster model  $G_k^{(T)}$  acts as a regularizer that preserves the generalizable knowledge learned through cross-cluster optimization, preventing catastrophic forgetting; (3) the KL divergence from the original client model  $f_i$  retains the client's pre-trained local knowledge that may be lost during cluster-level distillation.

## IV. EXPERIMENTS

### A. Experimental Setup

1) *Datasets:* We evaluate our method on four MedMNIST datasets [18]: BloodMNIST, DermaMNIST, OCTMNIST, and TissueMNIST. To simulate data heterogeneity, we partition the dataset using a Dirichlet distribution  $\text{Dir}(\alpha)$  with concentration parameter  $\alpha \in \{0.1, 0.2, 0.3, 0.5\}$ , where lower  $\alpha$  indicates higher heterogeneity. We consider three client settings:  $N = 5$  with  $K \in \{2, 3, 4\}$  clusters,  $N = 10$  with  $K \in \{3, 4, 5\}$ , and a larger-scale setting with  $K \in \{3, 5, 8\}$ . In the latter, we use  $N = 20$  clients for all datasets except DermaMNIST, which uses  $N = 15$  due to its smaller sample size.

2) *Baselines:* We compare against five one-shot FL baselines: FedAvg with a single communication round (FedAvg-1) [1], DAFL [19], DENSE [3], FedISCA [4], and Co-Boosting [5]. All methods are evaluated by test accuracy on each client, and we report the averaged accuracy across clients.

---

### Algorithm 1: FedBiCross

---

**Input:** Client models  $\{f_i\}_{i=1}^N$ , private datasets  $\{\mathcal{D}_i\}_{i=1}^N$ , clusters  $K$ , iterations  $T$   
**Output:** Personalized models  $\{f_i^{\text{pers}}\}_{i=1}^N$   
// Stage 1: Clustering & Data Generation  
1 Generate random noise images  $\{\mathbf{z}_m\}_{m=1}^M$ ;  
2 Compute prediction matrices  $\mathbf{p}_i$  for each client  $i$ ;  
3 Cluster clients into  $\{\mathcal{C}_k\}_{k=1}^K$  via  $K$ -means on  $\{\mathbf{p}_i\}$ ;  
4 **for**  $k = 1$  **to**  $K$  **do**  
5     Initialize synthetic data  $\hat{\mathbf{x}}_k^{(0)} \sim \mathcal{N}(0, 1)$ ;  
6     Construct ensemble teacher  $F_k$ ;  
7     **for**  $t = 1$  **to**  $T$  **do**  
8         Update  $\hat{\mathbf{x}}_k^{(t)}$  via Eq. (1);  
9         Construct noise-adapted teacher  $\tilde{F}_k$  via Eq. (3);  
// Stage 2: Bi-Level Optimization  
10 **for**  $k = 1$  **to**  $K$  **do**  
11     Initialize cluster model  $G_k^{(0)}$  randomly;  
12     Initialize cross-cluster weights  $\mathbf{w}_k^{(0)} \leftarrow \mathbf{1}/K$ ;  
13     **for**  $t = 1$  **to**  $T$  **do**  
14         Update  $G_k^{(t)}$  using inner optimization (Eq. 7);  
15         Update  $\mathbf{w}_k^{(t)}$  via outer optimization (Eq. 8);  
// Stage 3: Personalized Distillation  
16 **for**  $k = 1$  **to**  $K$  **do**  
17     **for**  $i \in \mathcal{C}_k$  **do**  
18         Initialize  $f_i^{\text{pers}} \leftarrow G_k^{(T)}$ ;  
19         Fine-tune  $f_i^{\text{pers}}$  on local data  $\mathcal{D}_i$  via Eq. (9);  
20 **return**  $\{f_i^{\text{pers}}\}_{i=1}^N$

---

3) *Implementation Details:* We adopt ResNet-18 as the backbone. Client models are trained for 100 epochs using SGD with learning rate  $10^{-3}$  and batch size 128. For client clustering, we use  $M = 256$  random noise images to compute prediction matrices. For synthetic data generation, we optimize inputs for  $T = 500$  iterations with batch size  $B = 256$  using Adam with learning rate  $5 \times 10^{-2}$ , where 80% of samples are used for training and 20% for validation in bi-level optimization. We set  $\alpha_{\text{TV}} = 2.5 \times 10^{-5}$ ,  $\alpha_{\text{BN}} = 10$ , temperature  $\tau = 20$ , and momentum  $\beta = 0.9$  for noise adaptation. For personalized distillation, we set  $\gamma = 0.5$ ,  $\delta = 0.3$  and fine-tune for 10 epochs.

### B. Main Results

Tables I, II, and III summarize results on four MedMNIST datasets under different client counts and heterogeneity levels. FedBiCross consistently attains the best accuracy and yields substantial gains over the strongest competing method. On BloodMNIST with  $N = 5$  and  $\alpha = 0.1$ , FedBiCross achieves 85.57%, surpassing Co-Boosting (54.75%) by 30.82%. Under increased heterogeneity (as  $\alpha$  drops from 0.5 to 0.1), Co-Boosting degrades from 80.32% to 54.75%, while FedBiCross



TABLE I  
COMPARISON OF DIFFERENT METHODS ON VARIOUS DATASETS WITH  $N = 5$  CLIENTS AND DIFFERENT HETEROGENEITY LEVELS (ACCURACY%)

Method	BloodMNIST				DermaMNIST				OCTMNIST				TissueMNIST				
	0.1	0.2	0.3	0.5	0.1	0.2	0.3	0.5	0.1	0.2	0.3	0.5	0.1	0.2	0.3	0.5	
Baseline	FedAvg-1	14.23	16.37	17.35	18.26	15.62	16.48	17.24	64.62	28.86	30.34	31.10	33.75	29.78	31.45	33.76	34.08
	DAFL	13.42	14.05	15.74	17.03	15.96	16.86	17.71	66.31	27.39	29.12	31.58	36.74	29.33	31.56	35.01	45.78
	DENSE	42.34	46.78	50.45	75.78	16.85	17.60	18.45	66.56	49.72	51.46	54.32	61.83	28.78	31.71	33.88	40.63
	FedISCA	48.49	50.64	53.28	79.83	18.12	19.89	21.84	68.05	52.05	56.26	60.47	67.58	43.81	44.98	49.86	52.15
	Co-Boosting	54.75	56.16	58.41	80.32	38.29	43.55	46.08	67.40	51.78	54.90	57.63	65.77	48.92	51.03	53.26	56.03
Ours	Ours ( $K=2$ )	84.94	86.51	87.15	88.65	65.17	67.03	68.12	<b>73.21</b>	61.95	63.78	66.62	<b>71.36</b>	61.28	62.75	63.71	<b>65.02</b>
	Ours ( $K=3$ )	83.31	83.90	<b>87.67</b>	<b>90.13</b>	<b>65.82</b>	<b>69.66</b>	<b>71.45</b>	71.29	<b>63.77</b>	<b>65.42</b>	<b>68.01</b>	70.12	60.03	<b>63.97</b>	<b>64.81</b>	64.21
	Ours ( $K=4$ )	<b>85.57</b>	<b>87.12</b>	85.63	86.17	64.52	68.40	67.22	71.18	60.86	64.14	67.23	69.88	<b>62.54</b>	62.52	64.60	64.97
Ablation	Intra-cluster	80.01	81.75	83.07	85.92	60.08	64.11	66.12	69.10	56.56	61.78	65.56	68.22	60.28	61.99	63.90	63.98
	Uniform cross	81.66	83.35	84.44	86.17	61.79	65.76	67.30	70.13	58.71	63.46	65.98	69.06	60.95	62.58	64.17	64.21
	Sim-weighted	82.99	83.63	85.13	87.02	63.05	66.08	67.44	71.16	59.42	63.80	66.41	69.64	61.49	62.64	64.39	64.42
	w/o PKD	77.69	79.52	81.15	84.16	57.69	61.80	65.31	73.05	53.56	59.43	63.12	68.33	59.34	61.17	63.52	64.39
	w/o Clus	76.47	76.41	78.40	82.64	51.28	56.64	59.35	69.09	53.03	58.32	62.19	68.07	56.61	58.50	59.74	60.11

TABLE II  
COMPARISON OF DIFFERENT METHODS ON VARIOUS DATASETS WITH  $N = 10$  CLIENTS AND DIFFERENT HETEROGENEITY LEVELS (ACCURACY%)

Method	BloodMNIST				DermaMNIST				OCTMNIST				TissueMNIST				
	0.1	0.2	0.3	0.5	0.1	0.2	0.3	0.5	0.1	0.2	0.3	0.5	0.1	0.2	0.3	0.5	
Baseline	FedAvg-1	13.58	14.95	16.28	17.41	14.92	15.86	16.44	61.85	27.84	29.41	30.22	32.96	28.66	30.78	33.01	33.54
	DAFL	12.74	13.31	14.73	16.07	15.18	15.96	17.74	60.62	26.52	27.98	29.57	33.88	26.89	30.75	32.29	41.97
	DENSE	38.62	40.73	45.12	64.45	16.09	16.91	17.63	63.18	48.97	50.55	53.46	57.92	27.12	29.84	33.02	37.72
	FedISCA	44.28	45.97	48.60	74.31	17.43	19.03	20.88	64.63	51.28	54.66	57.34	63.20	39.76	42.04	47.38	51.87
	Co-Boosting	49.52	52.67	54.10	72.89	35.63	40.76	43.21	63.28	50.67	53.82	55.38	61.04	43.88	46.63	49.94	54.28
Ours	Ours ( $K=3$ )	77.59	80.37	81.61	<b>86.55</b>	62.18	64.48	68.29	<b>71.08</b>	61.18	63.56	<b>67.69</b>	<b>69.11</b>	57.13	59.05	61.37	<b>63.38</b>
	Ours ( $K=4$ )	78.67	<b>82.04</b>	<b>84.13</b>	84.26	<b>63.84</b>	<b>66.20</b>	<b>69.93</b>	70.26	<b>62.68</b>	<b>65.04</b>	66.81	65.89	58.79	60.57	<b>62.73</b>	62.10
	Ours ( $K=5$ )	<b>79.67</b>	81.90	82.04	85.60	61.01	65.20	69.11	69.97	62.11	63.47	66.83	67.36	<b>59.11</b>	<b>61.25</b>	61.82	62.45
Ablation	Intra-cluster	72.91	75.41	77.93	80.56	59.41	62.26	65.35	67.40	58.29	59.72	64.40	63.76	53.72	56.18	58.49	60.17
	Uniform cross	75.14	77.52	79.81	82.18	60.88	62.75	66.97	68.15	59.41	60.90	65.31	64.23	55.45	57.91	60.07	60.79
	Sim-weighted	76.23	78.56	80.85	83.45	60.92	64.10	68.01	69.03	60.88	60.94	66.86	65.04	56.72	58.04	60.22	61.83
	w/o PKD	67.26	71.26	74.48	75.89	51.03	55.63	59.87	66.68	54.14	57.87	61.62	64.09	53.51	57.28	59.66	61.31
	w/o Clus	65.48	70.41	73.08	74.76	50.92	53.71	56.89	65.21	53.95	58.07	59.71	65.95	51.89	54.14	57.13	60.28

remains robust (90.13% to 85.57%), preserving the performance margin. The trend persists in larger client settings. With  $N = 20$  and  $\alpha = 0.1$ , FedBiCross attains 66.73%, outperforming Co-Boosting (37.09%) by 29.64%. We further observe that increasing the cluster number  $K$  improves performance under high heterogeneity, indicating a trade-off between intra-cluster coherence and data sufficiency.

### C. Ablation Study

The ablations in Tables I–III verify the effect of each component. For cross-cluster knowledge utilization, bi-level optimization is consistently best. On BloodMNIST with  $N = 5$  and  $\alpha = 0.1$ , intra-cluster reaches 80.01%, uniform weighting 81.66%, similarity weighting 82.99%, and learned weights 85.57%, showing that adaptive cross-cluster weighting surpasses heuristic designs. Removing personalized distillation (w/o PKD) yields large drops, such as 63.84% to 51.03% on DermaMNIST with  $N = 10$ , indicating that cluster models alone fail to capture client-specific patterns. Removing clustering (w/o Clus) degrades performance further, such as 53.68% to 48.72% on TissueMNIST with  $N = 20$ , since the lack of clustering and bi-level optimization prevents personalized distillation from obtaining strong global teachers.

We also ablate clustering in Fig. 2. [20] (“K-Means”) clusters model parameters via K-Means; [10] (“HC”) uses hierarchical clustering. PACFL [12] clusters clients using subspaces from local data via truncated SVD, requiring data-dependent transmission and increasing privacy risk. FedBiCross instead infers client label distributions from uploaded models alone, without extra transmission, while achieving comparable performance.

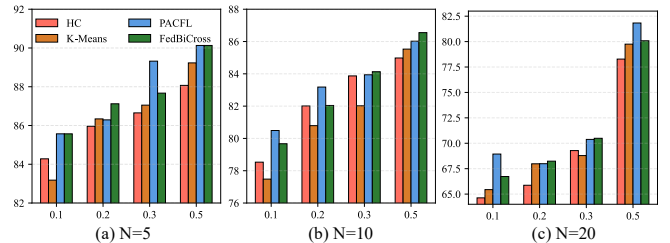


Fig. 2. Ablation on the clustering stage for BloodMNIST. Test accuracy (%) under varying client numbers  $N$  and heterogeneity levels  $\alpha$ .

### D. Synthetic Data Quality

Figure 3 visualizes synthetic images generated by different methods under non-IID settings. DAFL suffers from mode

TABLE III  
COMPARISON OF DIFFERENT METHODS ON VARIOUS DATASETS IN THE LARGE-CLIENT SETTING WITH VARYING HETEROGENEITY (ACCURACY%)

Method	BloodMNIST				DermaMNIST				OCTMNIST				TissueMNIST				
	0.1	0.2	0.3	0.5	0.1	0.2	0.3	0.5	0.1	0.2	0.3	0.5	0.1	0.2	0.3	0.5	
Baseline	FedAvg-1	12.95	13.70	14.01	15.28	14.76	15.23	14.85	58.44	25.98	27.65	27.81	29.40	22.43	24.82	26.19	29.24
	DAFL	12.55	12.83	13.17	14.29	14.55	14.96	16.57	57.40	25.43	26.97	28.22	31.58	20.96	23.77	25.49	36.86
	DENSE	29.90	32.46	34.16	65.85	15.24	15.89	16.33	58.25	46.89	48.11	50.57	55.98	22.90	24.66	27.92	30.85
	FedISCA	31.47	36.50	42.89	72.52	17.02	17.85	18.91	60.42	49.30	52.84	53.27	58.75	32.56	35.87	41.96	48.24
	Co-Boosting	37.09	43.81	48.97	70.35	31.22	35.28	38.60	60.59	47.81	51.68	52.84	56.53	37.43	38.10	43.48	49.78
Ours	Ours ( $K=3$ )	64.65	67.18	68.34	<b>80.08</b>	51.14	53.46	<b>58.46</b>	<b>67.10</b>	59.82	62.96	65.68	<b>68.14</b>	52.22	53.89	56.74	<b>59.56</b>
	Ours ( $K=5$ )	64.88	<b>68.24</b>	<b>70.49</b>	77.92	<b>52.61</b>	<b>55.85</b>	57.07	65.58	<b>61.26</b>	<b>64.33</b>	<b>67.07</b>	67.71	52.86	<b>55.21</b>	<b>57.09</b>	59.19
	Ours ( $K=8$ )	<b>66.73</b>	65.41	68.71	76.50	50.73	52.98	56.62	65.03	59.88	63.40	66.11	67.68	<b>53.68</b>	54.09	55.31	58.70
Ablation	Intra-cluster	61.21	63.54	65.14	73.74	47.12	49.98	53.83	63.57	57.84	59.63	63.61	64.98	49.61	51.22	54.68	58.12
	Uniform cross	61.49	66.02	65.33	74.88	48.36	49.11	55.06	64.14	57.08	60.92	63.96	65.11	50.83	52.44	55.23	58.33
	Sim-weighted	63.86	66.90	67.71	76.32	50.12	52.42	55.71	64.62	59.46	62.37	65.21	67.08	52.17	52.61	55.88	58.52
	w/o PKD	54.62	58.85	61.47	72.89	41.32	46.61	49.45	63.93	51.18	54.25	56.32	59.91	46.24	49.63	54.07	57.90
	w/o Clus	53.73	58.28	62.14	73.64	43.18	46.77	51.06	64.73	50.67	55.76	57.08	60.36	48.72	50.89	53.96	56.74

collapse, producing nearly blank images. DENSE generates blurry images lacking clear structure. FedISCA shows improved structure but exhibits stripe artifacts, particularly on OCTMNIST. Co-Boosting produces images with chaotic patterns and unnatural colors. In contrast, our cluster-specific generation yields more recognizable medical features, such as cell structures in BloodMNIST and TissueMNIST, demonstrating that coherent sub-ensembles mitigate teacher conflicts.

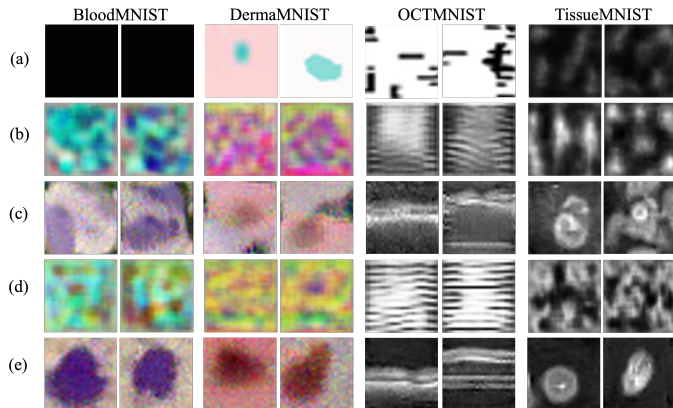


Fig. 3. Visualization of synthetic images generated by different methods under non-IID settings with  $\alpha = 0.3$  and  $N = 10$ : (a) DAFL, (b) DENSE, (c) FedISCA, (d) Co-Boosting, and (e) Ours.

## V. CONCLUSION

We presented FedBiCross, a personalized one-shot federated learning framework for non-IID medical data. By identifying that teacher disagreement causes near-uniform soft labels under heterogeneous distributions, we proposed client clustering based on model output similarity to form coherent sub-ensembles, and bi-level optimization to learn adaptive cross-cluster weights. Experiments on four medical imaging datasets validated that FedBiCross significantly outperforms existing methods, demonstrating that addressing teacher conflicts through clustering and controlled cross-cluster knowledge utilization is essential for OSFL in medical scenarios.

## REFERENCES

- [1] Brendan McMahan, Eider Moore, Daniel Ramage, Seth Hampson, and Blaise Aguera y Arcas, "Communication-efficient learning of deep networks from decentralized data," in *AISTATS*, 2017, pp. 1273–1282.
- [2] Neel Guha, Ameet Talwalkar, and Virginia Smith, "One-shot federated learning," *arXiv preprint arXiv:1902.11175*, 2019.
- [3] Jie Zhang, Chen Chen, Bo Li, Lingjuan Lyu, Shuang Wu, Shouhong Ding, Chunhua Shen, and Chao Wu, "Dense: Data-free one-shot federated learning," *NeurIPS*, vol. 35, pp. 21414–21428, 2022.
- [4] Myeongkyun Kang, Philip Chikontwe, Soopil Kim, Kyong Hwan Jin, Ehsan Adeli, Kilian M Pohl, and Sang Hyun Park, "One-shot federated learning on medical data using knowledge distillation with image synthesis and client model adaptation," in *MICCAI*, 2023, pp. 521–531.
- [5] Rong Dai, Yonggang Zhang, Ang Li, Tongliang Liu, Xun Yang, and Bo Han, "Enhancing one-shot federated learning through data and ensemble co-boosting," in *ICLR*, 2024.
- [6] Hongxu Yin, Pavlo Molchanov, Jose M Alvarez, Zhizhong Li, Arun Mallya, Derek Hoiem, Niraj K Jha, and Jan Kautz, "Dreaming to distill: Data-free knowledge transfer via deepinversion," in *CVPR*, 2020, pp. 8715–8724.
- [7] Jian Xu, Xinyi Tong, and Shao-Lun Huang, "Personalized federated learning with feature alignment and classifier collaboration," in *ICLR*, 2023.
- [8] Jaehoon Oh, Sangmook Kim, and Se-Young Yun, "Fedbabu: Towards enhanced representation for federated image classification," in *ICLR*, 2022.
- [9] Pouya M Ghari and Yanning Shen, "Personalized federated learning with mixture of models for adaptive prediction and model fine-tuning," *NeurIPS*, vol. 37, pp. 92155–92183, 2024.
- [10] Christopher Briggs, Zhong Fan, and Peter Andras, "Federated learning with hierarchical clustering of local updates to improve training on non-iid data," in *IJCNN*, 2020, pp. 1–9.
- [11] Avishek Ghosh, Jichan Chung, Dong Yin, and Kannan Ramchandran, "An efficient framework for clustered federated learning," *NeurIPS*, vol. 33, pp. 19586–19597, 2020.
- [12] Saeed Vahidian, Mahdi Morafah, Weijia Wang, Vyacheslav Kungurtsev, Chen Chen, Mubarak Shah, and Bill Lin, "Efficient distribution similarity identification in clustered federated learning via principal angles between client data subspaces," in *AAAI*, 2023, vol. 37, pp. 10043–10052.
- [13] Anirudh Kasturi, Anish Reddy Ellore, and Chittaranjan Hota, "Fusion learning: A one shot federated learning," in *International Conference on Computational Science*, 2020, pp. 424–436.
- [14] Youxingzhu Deng, Yipeng Zhou, Gang Liu, Jessie Hui Wang, and Yu Shui, "Enhancing federated learning by one-shot transferring of intermediate features from clients," in *DSAA*, 2023, pp. 1–11.
- [15] Yanlin Zhou, George Pu, Xiyao Ma, Xiaolin Li, and Dapeng Wu, "Distilled one-shot federated learning," *arXiv preprint arXiv:2009.07999*, 2020.

- [16] Clare Elizabeth Heinbaugh, Emilio Luz-Ricca, and Huajie Shao, “Data-free one-shot federated learning under very high statistical heterogeneity,” in *ICLR*, 2023.
- [17] Yufei Ma, Hanwen Zhang, Qiya Yang, Guibo Luo, and Yuesheng Zhu, “A new one-shot federated learning framework for medical imaging classification with feature-guided rectified flow and knowledge distillation,” in *ECAI*, 2025.
- [18] Jiancheng Yang, Rui Shi, Donglai Wei, Zequan Liu, Lin Zhao, Bilian Ke, Hanspeter Pfister, and Bingbing Ni, “Medmnist v2-a large-scale lightweight benchmark for 2d and 3d biomedical image classification,” *Scientific Data*, vol. 10, no. 1, pp. 41, 2023.
- [19] Hanting Chen, Yunhe Wang, Chang Xu, Zhaohui Yang, Chuanjian Liu, Boxin Shi, Chunjing Xu, Chao Xu, and Qi Tian, “Data-free learning of student networks,” in *ICCV*, 2019, pp. 3514–3522.
- [20] Avishek Ghosh, Justin Hong, Dong Yin, and Kannan Ramchandran, “Robust federated learning in a heterogeneous environment,” *arXiv preprint arXiv:1906.06629*, 2019.